Molding and Replication of Ceramic Surfaces with Nanoscale Resolution**

*Maria A. Auger, Patricia L. Schilardi, Ignacio Caretti, Olga Sánchez, Guillermo Benítez, José M. Albella, Raúl Gago, Mariano Fonticelli, Luis Vázquez, Roberto C. Salvarezza, and Omar Azzaroni**

***T**he design of reproducible and more efficient nanofabrication routes has become a very active research field in recent years. In particular, the development of new methods for micro- and nanopatterning materials surfaces has attracted the attention of many researchers in industry and academia as a consequence of the growing relevance of patterned surfaces in many technological fields, ranging from optoelectronics to biotechnology. In this work we explore, discuss, and demonstrate the possibility of extending the well-known molding and replication strategy for patterning ceramic materials with nanoscale resolution. To achieve this goal we have combined physical deposition methods, molecule-thick anti-sticking coatings, and nanostructured substrates as master surfaces. This new perspective on an "old technology", as molding is, provides an interesting alternative for high-resolution, direct surface-relief patterning of materials that currently requires expensive and time-consuming lithographic approaches.*

Keywords:
- ceramics
- micromachining
- molding
- nanotechnology
- patterning

The design and development of novel and reproducible strategies for nano- and microscale patterning of materials surfaces has become one of the most relevant topics in emerging nanotechnology.[1] For example, it is possible to modify the efficiency of a solar cell by introducing a determined surface-relief pattern onto the semiconducting substrate[2] or tailoring the antireflective properties of polymeric materials by nanopatterning their surfaces.[3] In order to achieve this goal many patterning methods with different degrees of accuracy have been developed during the last decade. In many cases, interesting patterning approaches were not able to reach the presumed technological impact as a consequence of lacking the required combination of reproducibility, accuracy, simplicity, and more important, suitability for large-scale fabrication.

As is well known, researchers involved in the application and development of ceramic-based technologies work with the aim of minimizing the extremely high costs associated with the design, development, and large production of ceramic-based micro- and nanodevices. This fact has turned research on nanopatterning and nanomachining of ceramics and hard materials into a frontier topic of the current nanotechnologies. Ceramic materials combine properties that make them extremely well suited for manufacturing diverse miniaturized devices, such as the microelectromechanical systems.[4–7] In the beginning, the most commonly used approaches for patterning hard material and ceramic surfaces were the hard-lithographic techniques,[8–10] that in many cases are time-consuming, expensive, and/or low-resolution techniques. Focused ion-beam lithography has been widely

[*] Dr. P. L. Schilardi, Dr. G. Benítez, Dr. M. Fonticelli, Dr. R. C. Salvarezza, Dr. O. Azzaroni
Instituto de Investigaciones Fisicoquímicas Teóricas y Aplicadas (INIFTA)
Universidad Nacional de La Plata—CONICET
C.C. 16—Suc. 4 (1900) La Plata (Argentina)
Fax: (+54) 221-425-4642
E-mail: azzaroni@inifta.unlp.edu.ar
Dr. M. A. Auger, I. Caretti, Dr. O. Sánchez, Dr. J. M. Albella, Dr. R. Gago, Dr. L. Vázquez
Instituto de Ciencia de Materiales de Madrid (CSIC)
Sor Juana Inés de la Cruz 3, 28049, Madrid (Spain)
Dr. R. Gago
Centro de Microanálisis de Materiales, Universidad Autónoma de Madrid, Cantoblanco, E-28049, Madrid (Spain)

[**] We acknowledge financial support from ANPCyT PICT 02-11111 (Argentina), MAT 2002-04037-C03-03 and BFM 2003-07749-C05-02 from Ministerio de Educación y Ciencia (Spain), and the CONICET-CSIC cooperation program. M.A. acknowledges financial support from the European Community (G5RD-CT-2000-00333). O.A. acknowledges a grant from Fundación Antorchas (Argentina).

  DOI: 10.1002/smll.200400073

used for surface patterning of diamond and diamond-like materials.[11] Lately, laser micromachining has been the chosen technique for patterning hard ceramics such as Al_2O_3/TiC,[12] GaN,[10] or AlN.[13]

With this focus, the development of new alternative lithographic techniques for nanopatterning ceramic surfaces in an accurate manner by a low-cost and straightforward route is a technological goal with tremendous impact in many production processes ranging from traditional CD and DVD manufacturing to novel nanoimprinting-based technologies.[14] One outstanding alternative to the conventional hard-lithographic techniques for patterning ceramic materials was provided by soft lithography.[15,16] By means of molding techniques using rubber stamps, that is, polydimethylsiloxane (PDMS), it has been possible to transfer surface-relief patterns on ceramic materials. In general, the micromolded material was not the ceramic material itself but polymeric precursors,[17] ceramic suspensions,[18] or sol–gel precursors.[19] This promising soft lithographic approach has been solely implemented on the micrometer scale. However, one disadvantage of molding precursors is that post-molding treatments such as solvent evaporation or firing could introduce distortions due to shrinking effects on the desired sample.[20] This fact is a limiting point and a determinant factor when dealing with the molding of nanoscale features. Therefore, a further challenge on patterning and nanofabrication research consists on the adaptation of replica-molding techniques (that have been already used for other materials) to ceramics.

Molding technology could be interpreted as an "ancient strategy" with significant and unpredictable impact on next-generation nanotechnologies. Many research groups have demonstrated that the "traditional" concept of molding could be easily extended to the nanoworld.[14,21] Molding and replication are very simple strategies that are commonly used to transfer surface-relief patterns on diverse functional materials. The molding and replication approach[21] has demonstrated an ability to meet the requirements that serial fabrication demands (simple, high-resolution, low-cost, and high throughput). However, in spite of their outstanding advantages for transferring surface-relief patterns, replica-molding strategies have been almost exclusively used on polymeric materials.[15] In those cases, the relief-transfer process (molding) is mainly based on simple physical contact; it is carried out by casting a pre-polymer or polymer against a master surface. Then, after polymerization or solvent evaporation, the polymer film is released from the master. In the case of replication, it involves two consecutive "relief-transfer" processes. In the first process, a mold (negative replica) is prepared from the original master surface. In the second step, the mold is used to obtain the replica of the original surface. A somewhat similar technique is embossing, where a rigid master is pressed against a thermally softened thermoplastic polymer, in such a way as to imprint surface-relief structures onto it. At present, molding and replication techniques on polymer materials play a major role on large-scale fabrication of diffraction gratings, holograms, or compact discs. The possibility of extending the concept of molding and replication to other materials different from polymers would promote the technological impact of exploiting a very simple and straightforward route for patterning materials that currently involves the use of expensive and time-consuming hard-lithographic techniques.

An interesting route to explore is the direct molding of the ceramic material itself. In this alternative variation of the soft-lithographic approach of molding ceramic precursors, the ceramic material is directly deposited by physical methods on the mold or stamp, with no need for post-patterning treatments. In this case, the first relevant step of the molding process is to provide molds or stamps with good anti-sticking properties. In general, a low-surface-energy layer on mold surfaces not only helps the release process, but it also increases the mold lifetime by preventing further surface contamination. In this case, fluorine- or methyl-terminated self-assembled monolayers (SAMs) have been commonly used as anti-sticking layers during pattern transfer to polymeric materials due to their simplicity for building-up the release layer (self-assembly is a rather straightforward process).[22] Otherwise, the molecular thickness of the SAM enables conformal coverage of nanoscale features with no distortions due to the release layer thickness itself. The characteristics of the release layer depend sensitively on the chemical nature of the mold surface. In the case of silicon-made molds, alkylsilane SAMs act as very effective anti-sticking molecular coatings. The self-assembly process proceeds by immersing the silicon molds in a diluted solution of the SAM precursor, octadecyltrichlorosilane (OTS). The OTS molecules react with the hydroxy groups on the native oxide (grown spontaneously under ambient conditions) on the silicon mold. In the case of metallic molds, alkanethiolate SAMs are used instead of silanes. The alkanethiolate SAM is formed by immersing the metallic molds in a diluted alkanethiol solution; thus the organic molecules chemisorb (through the -SH terminal group) onto the mold metal surface.[23] In this way, alkanethiolate-modified metallic molds and silane-modified silicon molds have been used in our laboratory for patterning polymeric materials with 40-nm lateral and 6-nm vertical resolution.[24,25]

Recently, we showed that silane-modified silicon and alkanethiolate modified-metallic molds can be also used for large-scale direct patterning of metallic materials with sub-50-nm resolution.[26] In fact, by using this approach we were able to mold and to replicate nanometer-scale features into the surface of Au, Al, and Cu films deposited by thermal physical vapor deposition (PVD). A schematic representation of the procedure used to obtain molds and replicas by this method is shown in Scheme 1.

In this case, the temperature control was crucial to avoid damaging the self-assembled alkanethiolate (Figure 1) and silane monolayers (the anti-sticking layers) that must remain chemisorbed on the mold surface. Thus, the possibility to extend the approach shown in Scheme 1 for the direct patterning of ceramic materials appears particularly attractive. However, molding and replication of ceramic materials by depositing onto surface-modified molds is not so straightforward. It is well known that, in some cases, deposition conditions (temperature, particle energy) required to grow high-quality ceramic films can lead to severe damage of the

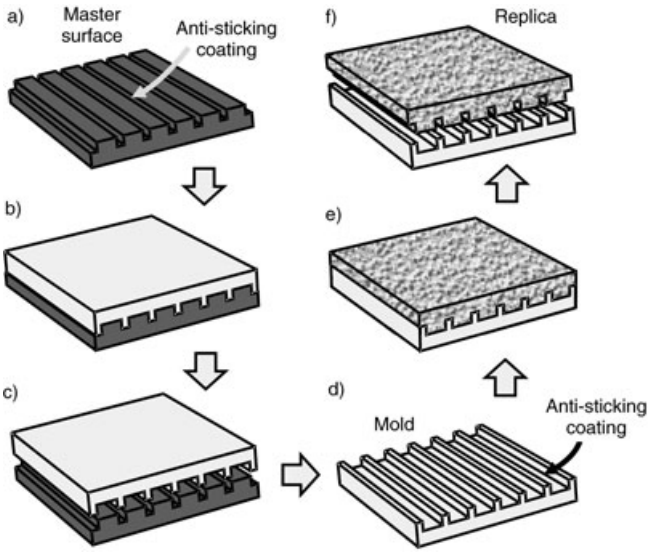

Scheme 1. The molding and replication procedure used for transferring surface-relief patterns. A master surface (a) modified with an anti-sticking coating is used to fabricate the corresponding metallic mold (b) by thermal evaporation. After deposition, the evaporated patterned film is released from the master (c) and is then modified with the anti-sticking coating (d). Afterwards, physical vapor deposition of the preset material is carried out on the surface-modified mold (e). Finally, the replica of the master surface is released from the mold (f).

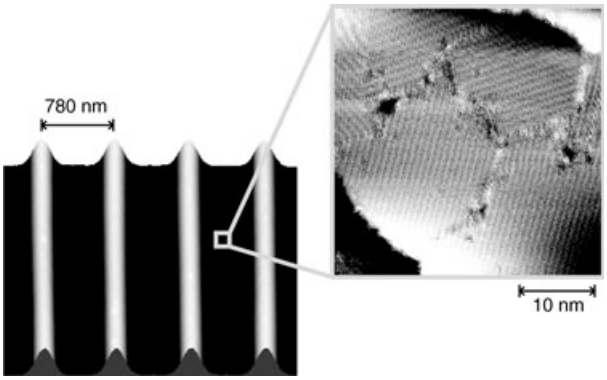

Figure 1. Scanning tunneling microscopy (STM) image ($3 \times 3\ \mu m^2$) of a surface-modified Au micromold obtained by thermal evaporation, as described in the text. The inset ($30 \times 30\ nm^2$) shows a STM image of the ordered arrays of the hexanethiol self-assembled monolayer (which acts as an anti-sticking layer) chemisorbed onto the evaporated Au surface.

self-assembled molecular film.[23,27] As a consequence, the release step during the molding procedure could fail.

These problems can be overcome by introducing slight changes in the deposition conditions. In the case of ceramic deposition by reactive sputtering, it is well known that this technique involves the formation of high-energy species such as ions, charged clusters, or electrons. Collision of these energetic species with the modified substrate produces immediate degradation of the SAM in the early stages of deposition.[27] However, these deleterious effects can be avoided by increasing the substrate-target distance (d), and by introducing an inert gas into the sputtering chamber, so as to "thermalize" the energetic species arriving at the SAM-modified substrate.

Once deposited, the patterned ceramic film is released from the mold. The "release step", that is, when the mold is separated from the master surface or the replica is separated from the mold (steps c and f in Scheme 1), is a procedure that demands particular attention in the replica molding of ceramic materials. In contrast to polymers, ceramics are brittle materials that can be severely damaged during the release step if some precautions with sample handling are not considered during the release procedure. In many cases, the use of small tweezers (similar to that used for manipulating microscope samples) results in damaging the thin sample as a consequence of the excessive pressure exerted by the tweezers tips. This problem can be easily avoided by releasing the deposited film using Scotch tape or by gluing the ceramic deposit to a glass substrate and then releasing the deposit from the micromold while holding the glass substrate with small tweezers.

With the aim of applying the molding concept to ceramics deposited by physical methods, we have studied, in particular, micromolding of aluminum nitride surfaces deposited by reactive sputtering on metallic micromolds. Aluminum nitride (AlN) is a ceramic material that exhibits a wide bandgap with potential applications in constructing arrays of electro-optical and photonic devices.[28] In spite of the promising properties of this ceramic material, little progress has been reported on the design of cost-effective and reproducible routes for the surface patterning of AlN. Wet-chemical etching routes[29] are not suitable for high-resolution processing of wide-bandgap semiconductors. Recently, excimer laser ablation has been proposed to fabricate patterned AlN surfaces in a "one-step" process.[28] However, this approach involves a one-by-one "writing" process for producing a large number of patterned samples; therefore, this route is very difficult to implement in large-scale fabrication. Another limitation related to AlN surface patterning by laser ablation that must be also taken into account is related to the chemical degradation of the material as a consequence of the thermal effect of laser pulses. Obara et al.[30] have shown that the use of micro- and nanosecond laser pulses produces Al-enriched domains as a result of AlN decomposition.

The ability to use a replica-molding approach for patterning materials such as AlN would provide a simple, cost-effective, and straightforward alternative to hard-lithographic techniques or wet-chemical etching routes. Such a strategy would be a valuable tool for surface patterning hard-to-micromachine materials.

We have used micromold surfaces made from copper (Figure 2a) that were easily surface-modified by immersion in a dodecanethiol solution (50 μM in toluene) for 12 h in order to allow the self-assembly of the dodecanethiolate species on the Cu surface.[31] The micromolds consisted of sinusoidal grating-like Cu surfaces (pitch $L = 730 \pm 10$ nm; amplitude $h = 107 \pm 3$ nm). The pitch of the sinusoidal pattern was estimated from the power spectral density (PSD) and Fourier analyses (FFT) of AFM images ($20 \times 20\ \mu m^2$

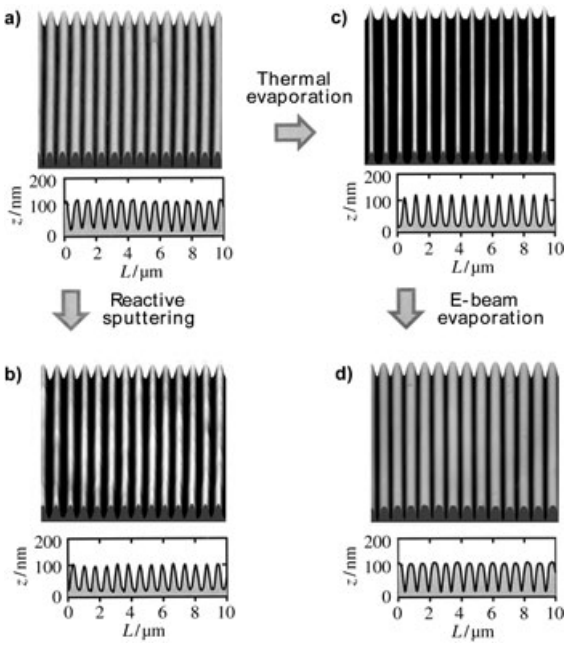

Figure 2. 10 × 10 μm² 3D AFM images and their corresponding cross sections showing: a) a Cu micromold; b) a micromolded AlN surface obtained by reactive sputtering onto the Cu micromold depicted in (a); c) a Au micromold obtained by thermal evaporation using the copper surface depicted in (a) as a master; d) a micromolded B_4C surface obtained by electron-beam evaporation onto the Au micromold depicted in (b).

scan size) rather than from cross-sectional analysis. Fourier analysis gives a more reliable value for the period (pitch) of the sinusoidal profile over the whole patterned surface than would local cross-sectional analysis in a predetermined region of the patterned substrate. Nonetheless, in our case, pitch values derived from cross-sectional analysis are in close agreement with those obtained from PSD and FFT analyses.

In our studies, AlN films were deposited onto the surface-modified Cu micromolds by dc reactive sputtering of a pure aluminum target under specific experimental conditions[32] that provide hard ceramic films (20% Ar + 80% N_2, total flux = 29.5 sccm, working pressure = 4×10^{-3} mbar). By the direct micromolding (deposition and release) of sputtered AlN films we have obtained AlN gratings by transferring surface-relief patterns from a metallic micromold to the inner face of the AlN film deposited onto it.

AFM imaging of the inner face of the AlN film (Figure 2b) shows a good-quality molded AlN surface. Cross-section analysis, in agreement with PSD and FFT analyses (not shown), indicates that the characteristic dimensions of the molded AlN samples are $L = 729 \pm 15$ nm and $h = 98 \pm 6$ nm, in accordance with the negative replica of the original patterned Cu surface (Figure 2a). Regarding the surface roughness, also measured parallel to the channels direction, only a slight increase in the rms roughness (3.5 nm < rms roughness < 4.0 nm) is observed on the patterned AlN surface with respect to the Cu micromold (3.0 nm < rms roughness < 3.5 nm).

During the sputtering experiments the target-to-substrate distance was $d = 26.5$ cm, larger than that currently used to grow ceramic materials in the same sputtering chamber to avoid damaging the micromold. In fact, reactive sputtering runs performed at $d = 6.5$ cm resulted in serious damage to the micromold due to the high-energy species impacting upon it. Other techniques for depositing ceramic films involve the evaporation of the ceramic material itself, such as electron-beam evaporation. In those cases, temperature is a relevant factor that could affect the stability of the anti-sticking coating. The evaporated particles arriving at the substrate are low-energy particles, thus proving no danger to SAM integrity. However, optical radiation from the evaporating source could raise the substrate temperature and promote thermal desorption or degradation of the molecular coating. Alkanethiolate SAMs on Au surfaces are desorbed at temperatures ≈100 °C by cleavage of the Au–S bond. In the case of alkanethiolate SAMs on Cu substrates, thermal desorption proceeds at ≈100 °C but by cleavage of the S–C bond. Finally, alkylsilane monolayers self-assembled on Si/SiO_2 are systems more resistant to temperature effects, being stable up to ≈460 °C.[23]

In our case, we have studied the micromolding of boron carbide (B_4C) films deposited by electron-beam evaporation on SAM-modified Au micromolds ($L = 718 \pm 10$ nm, $h = 107 \pm 4$ nm). These Au-molded surfaces (Figure 2c) were easily obtained by micromolding thermally evaporated gold films using copper micromolds similar to that depicted in Figure 2a as master surfaces. An incident 110 mA e-beam biased at 7 kV with a 1 cm^2 spot size was used to evaporate the B_4C films under vacuum conditions (10^{-5} mbar), thus melting pieces of commercial-grade B_4C contained in a water-cooled crucible. Thermal effects on SAM stability were minimized by increasing the evaporating source-substrate distance, thus diminishing the growing rate of the evaporated ceramic material but avoiding any damage to the anti-sticking coating. The substrate-to-target distance was fixed at 30 cm, in such a way that the substrate temperature remained below 100 °C at a growth rate of 0.2–0.3 nm s^{-1}. After depositing and releasing the B_4C films from the Au micromolds, the inner face of the deposited ceramic film clearly shows a surface topography in accordance to that expected (negative replica) from the mold structure (Figure 2d). Thus, the obtained micromolded B_4C surface resulted in a replica of the sinusoidal patterned Cu surface that was used the master surface. In this case, characteristic dimensions of the micromolded B_4C patterned samples, derived from cross-sectional analysis in combination with PSD and FFT, were $L = 737 \pm 10$ nm and $h = 104 \pm 5$ nm. These dimensions are in good agreement with those expected from Au micromolds.

It can be seen that neither AlN nor B_4C micromolded surfaces show significant shrinking effects. The amplitude of the sinusoidal relief structures transferred from the mold surface to the ceramic film suffers a shrinkage of < 5%, and the pitch shows only slight variations (< 2%). This is a clear advantage of the direct micromolding procedure if we consider that in most cases the micromolding of pre-ceramics or ceramic suspensions shows considerable isotropic or ani-

sotropic shrinkage after sintering or firing. Cao and coworkers observed that after firing micromolded $Sr_2Nb_2O_7$ sols, samples exhibited a shrinkage of $\approx 85\,\%$ in the vertical direction and negligible horizontal shrinkage.[33] Recently, Martin and Aksay demonstrated that the micromolding of sol–gel films could produce unintended topographical distortions from the shape of the original mold, with a consequence that during drying and heat treatment a non-uniform shrinkage across the micromolded film is observed.[34] This fact should limit the potential applications of the technique. Also, shrinkage has shown deleterious effects on micromolding ceramic suspensions where high drying shrinkage can lead to partial destruction of the patterned sample. This deleterious effect has been reduced (for ceramics patterning above the micrometer scale) by colloidal isopressing,[35] a technique in which a pre-consolidated slurry is injected into an elastomeric mold and isopressed to rapidly convert the slurry into an elastic body that can be released from the mold without any distortion.

A remarkable advantage of physical deposition methods such as sputtering or evaporation to grow the ceramic films is that compared to chemical routes, they easily produce deposits with small grain sizes (<30–40 nm). At early stages of deposition, the relief structures of the micromold are covered by small ceramic particles. Then, after further deposition, these small particles form a continuous ceramic film (with very small grain sizes) that is in conformal contact with the micromold surface, as is schematically shown in Scheme 2.

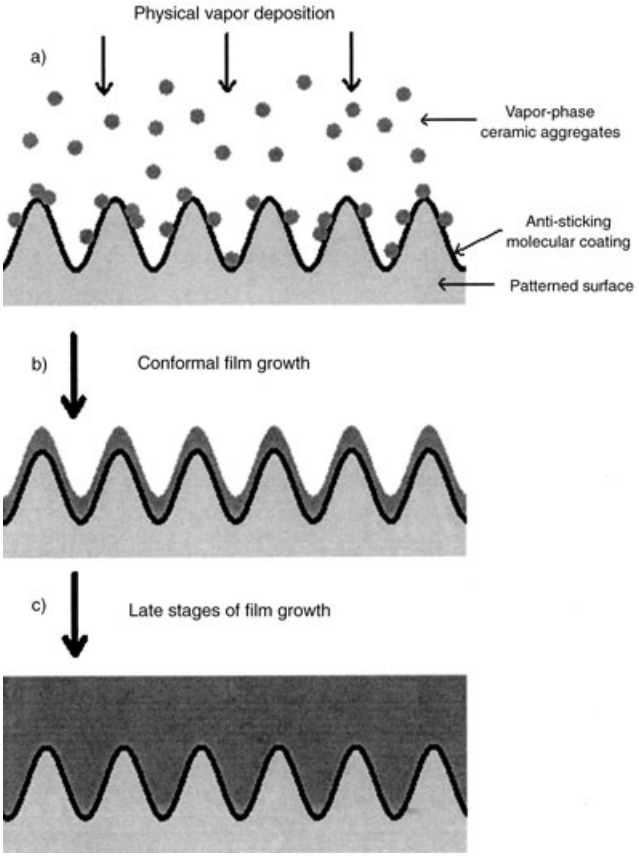

Scheme 2. The conformal thin-film growth process. a) In the early stages, small aggregates (not in scale) of the ceramic material are randomly deposited on the patterned surface; b) the patterned surface is then covered by a continuous ceramic thin film that is in conformal contact with the substrate; c) after further deposition a thick ceramic film is grown onto the patterned surface.

Direct micromolding involves the combination of conformal growth and small-grain-sized films. Conformal film growth during the initial stages of deposition is responsible for the high accuracy associated with the direct micromolding method. Thus, micromolded ceramic relief structures showing considerable low-edge roughness[36] are due to small grains acting as building blocks of the deposited film. This observation is in agreement with results reported by Schönholzer and Gauckler on the micromolding of ceramic suspensions.[37] They observed that particle size of the processed ceramic powders played a key role on pattern formation, where coarse powders exhibited a poorer pattern resolution than finer powders. In Figure 3 is depicted a micromolded titanium nitride (TiN) surface deposited by reactive sputtering ($L = 748 \pm 12$ nm, $h = 102 \pm 7$ nm) showing in detail the low edge-roughness and the small-sized grains (building blocks) forming the surface-relief structures along the substrate.

These low-roughness structures micromolded on TiN are very difficult to obtain by erosive techniques such as laser ablation, a technique commonly used for patterning ceramic and hard materials. Our interest on micromolding TiN films is based on their promising technological applications, such as building durable multiple-use master molds due to their hydrophobicity and chemical and mechanical stability. In our case, the quality of the micromolded surface-relief pattern is comparable to that recently reported using focused ion-beam lithography.[38]

Nano- and microstructured ceramic films exhibit high stability and hardness. We have obtained values in the range of 13–15 GPa for the hardness of patterned TiN films, irrespective of the presence of the OTS monolayer (Figure 4). This hardness is slightly less than that reported for the bulk ceramic material (18 GPa).[39] It should be noted that the measured hardness is only independent of the OTS layer by using a depth indentation less than 10 % of the TiN layer thickness. This fact is in close agreement with the results of Wittling et al., who stated that a reliable hardness measurement should involve a 10 % depth indentation in order to avoid substrate influence.[40] This effect is more clearly revealed for TiN films deposited on Cu substrates as shown in Figure 4.

Currently, there are many flourishing technologies based on nanoimprinting processes, such as those developed by Chou et al.,[14] that use hard-material stamps as an imprinting tool. For example, in the case of CD and DVD production, it has been suggested that replacement of the traditional Ni stamps with ceramic-based stamps would change drastically the production process due to the enhanced wear properties of the ceramic stamps.[41] Underscoring this suggestion, the hardness of patterned ceramic material is remarkably higher than that of SiO_2 (7–9 GPa),[42] a material currently used for building imprinting stamps.[5] We have

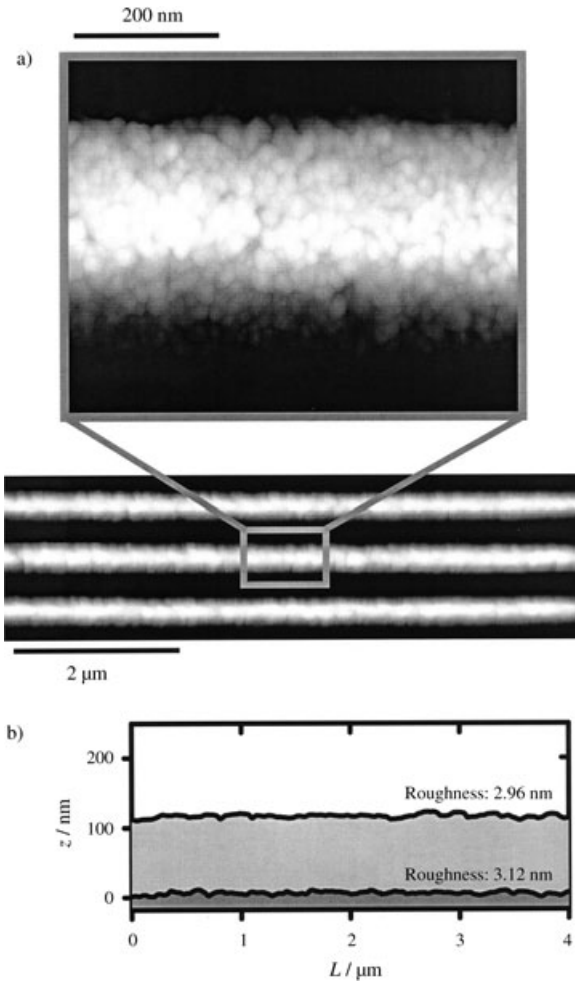

Figure 3. a) Top-view AFM image ($6 \times 2\ \mu m^2$) of a micromolded TiN film deposited by reactive sputtering. The inset shows in detail the small grain size of the micromolded ceramic deposit; b) cross-sectional analysis, including the roughness along the surface-relief structures, which shows that low roughness can be achieved by the direct-micromolding procedure.

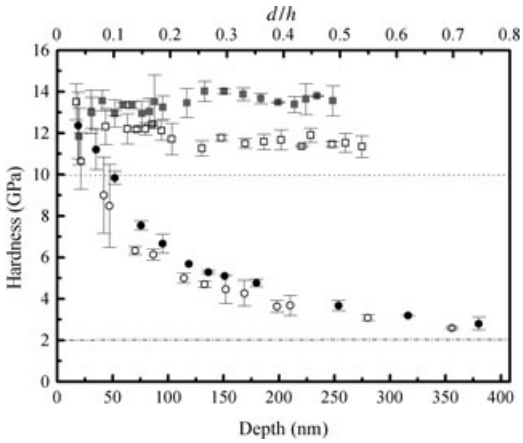

Figure 4. Plots of hardness as a function of penetration depth (lower *x* axis) and normalized penetration depth, d/h (top *x* axis), where d is the indentation depth and h is the total coating thickness for a 510-nm TiN layer on: a bare copper substrate (●), thiol-functionalized Cu (○), bare Si (■), and OTS-functionalized Si (□). The dashed horizontal lines indicate our reference measurements of the hardness for silicon (-----) and copper (–•–•).

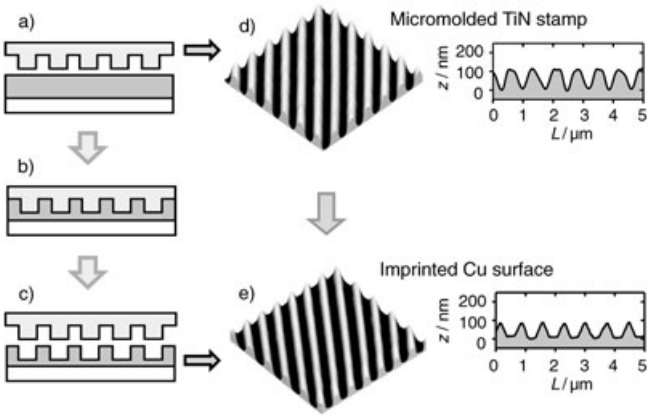

Figure 5. The imprinting procedure. a–c) First, the TiN stamp is placed on the evaporated Cu surface (a). Then, the stamp is pressed onto the metal substrate (b). Finally, the ceramic stamp is released from the imprinted Cu surface (c); d) 3D-AFM image ($6 \times 6\ \mu m^2$) of the micromolded TiN stamp and its corresponding cross section; e) 3D-AFM image ($6 \times 6\ \mu m^2$) of the imprinted Cu surface and its corresponding cross section.

tested the hardness and stability of micropatterned TiN films by using them as stamps for imprinting metallic surfaces.[43] The AFM image (Figure 5) shows a Cu (hardness = 2 GPa, Figure 4) surface imprinted with a TiN stamp fabricated by our procedure.

Imprinting experiments were performed at room temperature by pressing the TiN stamp into a 200-nm copper layer deposited on a glass substrate at 49 MPa over 2 h. Note the excellent pattern transfer from the TiN stamp to the Cu surface. The characteristic dimensions of the imprinted Cu substrate were $L = 728 \pm 10$ nm and $h = 89 \pm 5$ nm, which indicates some loss of relief height (h) on the imprinting process.

Most patterning methods suitable for ceramics and hard materials are limited to the micrometer scale. At present, there are very few reproducible techniques for patterning hard ceramic surfaces below this scale and even less under the 100-nm scale. Recently, some results on the large-scale patterning of silicon by using a laser-assisted direct-imprint technique have been reported.[44] In this technique, a laser pulse melts a thin layer of the silicon surface and a mold is embossed into the resulting liquid layer. Also in recent years, the group of Aksay has developed novel procedures based on self-assembly and the use of amphiphilic surfactants and block copolymers that have enabled them to form nanostructured silica films in an accurate manner.[45] Another interesting approach for-large scale nanopatterning of hard materials is the use of block-copolymer lithography. By using this approach it is possible to "write" a high density of nanostructures on a ceramic substrate.[46] More recently, Ruda and co-workers developed a method to achieve an accurate patterning of ceramics based on the combination of electron-beam lithography and metallopolymer resists.[47]

Under this focus, the idea of extending the concept of molding and/or replication to ceramic surfaces with nanoscale features appears as a simple and attractive alternative to producing nanopatterned surfaces of materials that are extremely hard to machine on the nanoscale by using traditional approaches.

To explore the resolution limits of direct molding on ceramic surfaces, we have used a nanostructured silicon master[48] with a surface array of short-range ordered nanodots (Figure 6a) prepared by Ar^+ bombardement (1.2 KeV, 0.24 mA). The dots are 40 nm in diameter (D) and 6 nm in height (h) with a dot density $\approx 10^{11}$ cm^{-2} (Figure 6b). The SiO_2 surface was chemically modified by immersion in OTS solution (7 mM in hexane) for 1 h.[26] Thus, the nanodotted sample is homogeneously covered by an anti-sticking coating with molecular thickness (1.5–1.8 nm), as clearly shown in Figure 7.

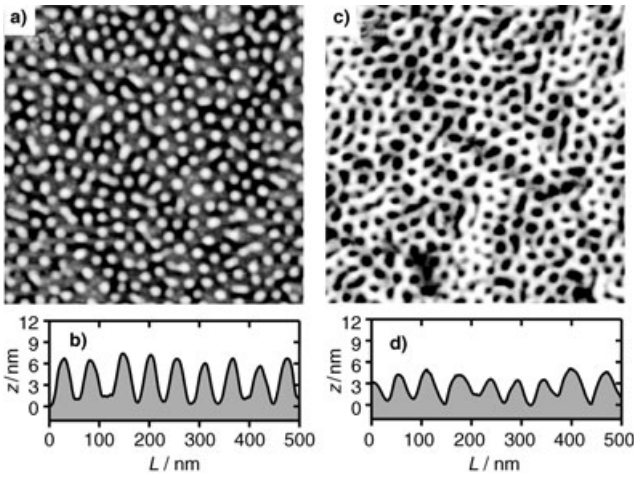

Figure 6. Top-view AFM images (1 × 1 μm^2) of a nanostructured SiO_2/Si surface (a) and a nanopatterned TiN surface (c), with associated cross-sectional analysis corresponding to the nanostructured SiO_2/Si (b) and the nanopatterned TiN surface (d).

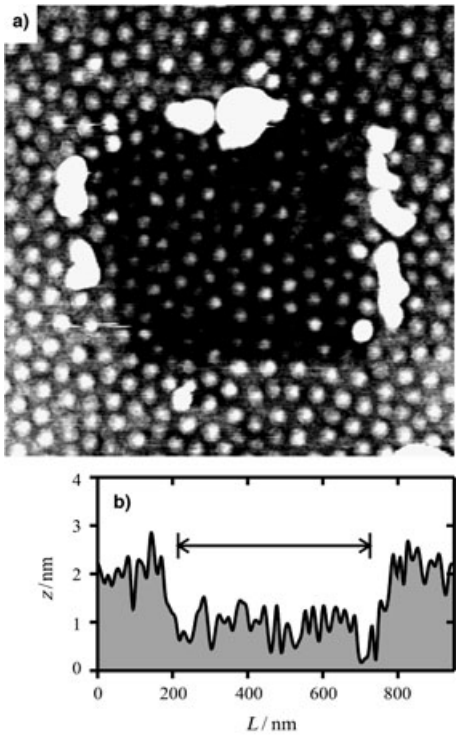

Figure 7. a) Tapping-mode AFM image (940 × 940 nm^2) and the corresponding cross section (b) of a region of an OTS-modified nanodotted SiO_2/Si substrate comprising a 500 × 500 nm^2 area (indicated by arrows) previously imaged with the same tip in contact mode at low load in order to remove the OTS layer.

We have used these nanostructured Si surfaces as molds for the direct nanomolding of ceramic surfaces. After depositing an 800-nm-thick TiN film by reactive sputtering, the inner face of the released ceramic film shows a large-scale surface patterning consisting of ordered arrays of nanoscale features (nanocavities; Figure 6c). The cross sections show the accurate manner in which the nanocavities were transferred to the ceramic surface (Figure 6d).

The geometry of the cavities is in close agreement with that expected from the size and shape of the nanostructured Si surface. The direct nanomolding process involved no distortions on lateral dimensions, as concluded from comparison of average nanodot and nanocavity diameters, both of which were $\approx$40 nm (as derived from cross sections in combination with PSD and auto-covariance analyses). Only slight variations in the z direction were observed (average dot height = 6 nm; average nanocavity depth = 4–5 nm). These depth differences could also be due, to some extent, to tip-convolution effects. It should be noted that it was not possible to image the ceramic/SAM/template interface by transmission electron microscopy (TEM) due to the spontaneous detachment of the ceramic film from the SAM-modified template during the sample preparation treatment.

Replication of nanodotted Si surfaces on different ceramic materials can also be achieved by a simple two-step procedure. In order to replicate the master surface we first built up a gold nanomold (negative replica; Figure 8a) of the original master surface. A 200-nm-thick gold film was deposited by thermal evaporation onto the OTS-modified nanodotted Si substrate. In general, to improve the mechanical stability of the mold, a 10-μm-thick copper layer was then electrodeposited on to it before releasing the gold nanomold from the Si/SiO_2 master.

The gold nanomolds were mechanically released from the OTS SAM-covered silicon masters by simply using small tweezers due to the excellent anti-adherent properties of the silane monolayers.[22] As expected, after releasing the inner interface of the gold film (that which was in contact with the OTS-covered silicon master), ordered arrays of nanocavities were observed. The corresponding cross sections show how the master features were transferred to the gold nanomold. Afterwards, these gold nanomolds were easily surface-modified by immersing them in a diluted dodecanethiolate solution (1–5 mM ethanolic solution during 6 h) and then used as substrates for further ceramic deposi-

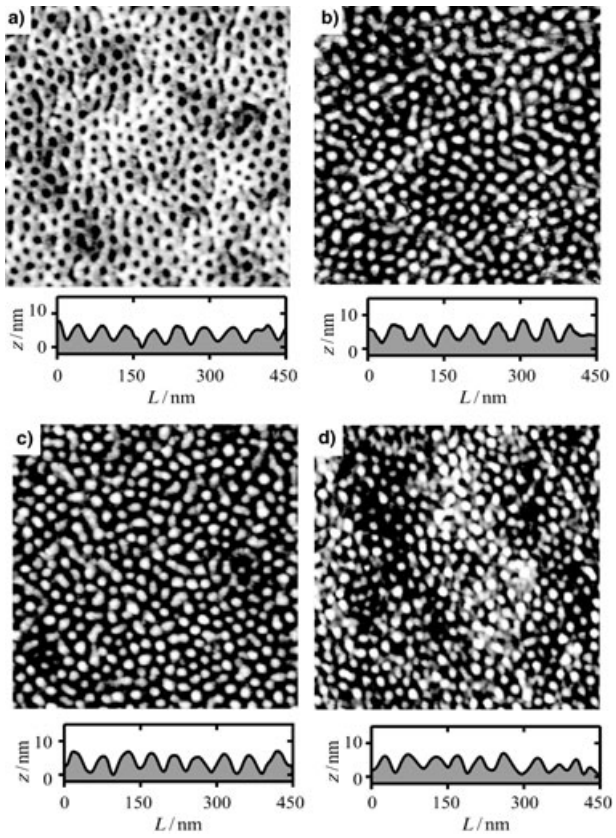

Figure 8. Top-view AFM images ($1.2 \times 1.2\ \mu m^2$) and their corresponding cross sections showing: a) a nanostructured Au mold; b) a nanomolded TiN surface; c) a nanomolded AlN surface; d) a nanostructured B_4C surface.

tion (TiN, AlN and B_4C) under previously described conditions. After deposition of ~1 μm thick ceramic films they were carefully released from the gold nanomolds taking into account the precautions described above.

AFM imaging of the inner face (that which was in contact with the SAM-modified gold nanomolds) of the released ceramic films showed nanostructured TiN (Figure 8b), AlN (Figure 8c), and B_4C (Figure 8d) surfaces consisting of arrays of nanodots with short-range hexagonal order that are replicas of the original nanostructured master Si surface. The corresponding cross sections show how accurately the mold features were transferred to the ceramic surfaces. The low roughness of the ceramic deposits (rms roughness ≈1.8 nm measured from AFM images; 2 μm^2 in size) is slightly higher than that (rms roughness ≈1.2 nm) measured from similar images taken on the gold nanomold. Thus, only a small increase in surface roughness occurs during ceramic deposition on the gold nanomold.

As previously stated, small grain size and low surface roughness are crucial to allow molding and replication with high resolution. Ceramic replicas show no significant evidence of shrinkage or dilation effects on lateral dimensions of surface features through the replication process. In all cases, we have performed PSD and FFT analyses of AFM images (scan size $15 \times 15\ \mu m^2$) of TiN, AlN, and B_4C nanostructured surfaces, which show that the obtained nanodots are ≈40 nm in diameter, in close resemblance to the original Si nanodots. However, slight variations in the height of the nanodots were observed; the original Si dots were 6 nm in height while the replicated ceramic nanodots were 3–5 nm high, indicating some loss in dot height after the nanoreplication procedure. In agreement with this observation, Xia et al.[21] reported similar master-replica variations for the replication of nanostructures on polymer materials. It should be noted that reliable pattern transfer with sub-10-nm vertical resolution is not a trivial task, in particular when dealing with materials that are very difficult to micro- or even nanomachine, as ceramics are. Recent results reported by Gates and Whitesides showed the capability of molding techniques in achieving 2-nm vertical resolution on polymer materials.[49] But, as is well known, the properties of polymers are completely different from those of ceramics. Thus, the possibility of achieving sub-10-nm vertical resolution on ceramic materials by using a molding approach is not straightforward. From this analysis it can be concluded that the resolution limits for this method are on the order of 40 nm and 6 nm for lateral and vertical dimensions, respectively. Otherwise, the capability of the direct nanorelief-transfer process is not solely restricted to one-step molding procedures but it can be extended to further replication (successive molding) steps, while preserving the accuracy and fidelity of each step.

In order to study the chemical composition of the ceramics, we have performed Rutherford backscattering spectroscopy (RBS) on nanostructured TiN samples. Figure 9 shows RBS spectra for TiN layers deposited on a bare silicon substrate and on a SAM-modified silicon surface. It can be noted that both spectra indicate a similar composition for the TiN layer (even the amount of oxygen contamination in the film), independent of the presence of the OTS layer. These results imply that the growth process is not altered by the addition of the anti-sticking monolayer.

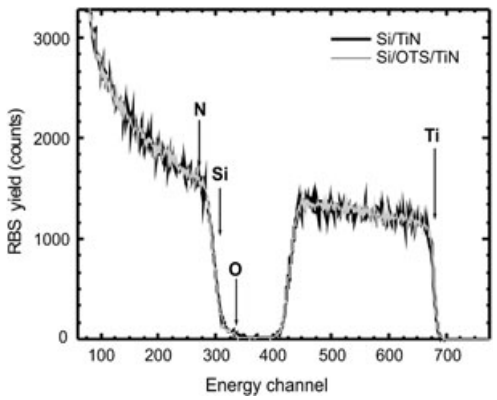

Figure 9. RBS spectra of TiN deposited on bare (black line) and OTS-modified (gray line) Si(100) substrates. The arrows indicate the start of the signal corresponding to each element. Ti, N, and O were detected from the sample surface whereas the Si signal comes from the substrate. It is evident that the addition of the OTS layer does not affect the composition of the TiN layer. Note that the N signal is not well resolved in the spectra due to the poor sensitivity of RBS to light elements and, in addition, the overlap with the Si signal from the substrate.

In addition, we have monitored by Auger electron spectroscopy (AES) the chemical composition of nanomold surfaces both before and after ceramic deposition. The surface chemical composition of dodecanethiolate-modified Au nanomolds is in agreement with the formation of a full monolayer (Figure 10a). Similar AES results on SAM-modified Au nanomolds were obtained after depositing and releasing the ceramic films (Figure 10b). This fact indicates that no contamination (within the detection limits of AES, ≈ 0.05 monolayers) of the metal nanomold occurs during the molding procedure. Otherwise, when nanostructured ceramic surfaces were analyzed no traces of alkanethiol (S signal) were detected, in agreement with RBS measurements (not shown). Figure 10c shows an AES spectrum of a nanostructured TiN, where no evidence of S on the sample surface can be observed.

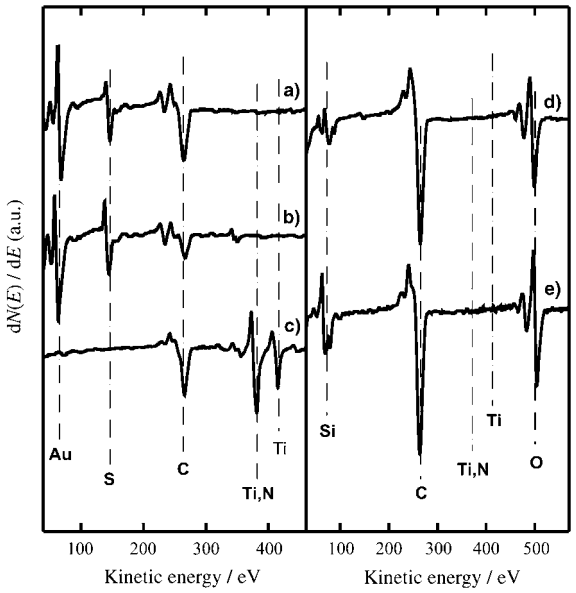

Figure 10. Auger electron spectra corresponding to the following surfaces: a) A dodecanethiolate-modified nanostructured Au mold prior to the reactive sputtering deposition of TiN films; b) a dodecanethiolate-modified nanostructured Au mold after depositing and releasing TiN films; c) a nanostructured TiN surface; d) an OTS-modified nanostructured Si/SiO_2 master prior to reactive sputtering deposition of TiN films; e) an OTS-modified nanostructured Si/SiO_2 master after depositing and releasing TiN films. Represented Auger signals correspond to: S (LVV, 152 eV), Au (NVV, 69 eV), C (KLL, 272 eV), O (KLL, 508 eV), Si (LVV, 91 eV), Ti (LMM, 387 eV, 418 eV), N (KLL, 380 eV).

A similar behavior was observed on nanomolding ceramic films by using nanostructured SiO_2/Si substrates as mold surfaces. For example, the chemical composition of the OTS-modified SiO_2/Si surfaces show just slight variations before (Figure 10d) and after (Figure 10e) TiN deposition, which indicates there was little alteration on the integrity of the OTS SAM. Besides, no ceramic traces (Ti and N) were detected on SiO_2/Si after releasing the TiN film. This clearly indicates that SAM-modified nanomolds can be reused for different deposition techniques, since no contamination on the nanostructured ceramic material is involved.

In conclusion, we have shown that molding and replication techniques based on molecular films as anti-adherent layers enable "large-scale" (on the order of cm^2) patterning of different ceramic materials with sub-50-nm resolution. The deposition conditions of the ceramic film on the surface-modified mold must be adjusted to avoid any damage on the self-assembled monolayer. In contrast to other template methods that involve etching or chemical dissolution of the original template to release the molded sample, replica-molding approaches using anti-sticking release layers involve no destructive steps. This method appears particularly attractive because it is relatively simple, straightforward, and inexpensive, and accordingly, can be used as an alternative route to the conventional lithographic techniques. It is likely that ongoing work following this route could improve the patterning scale in such a way so that CD-sized (i.e., several cm^2) ultrahard nanostructured molds could be envisioned.

[1] *Alternative Lithography: Unleashing the Potentials of Nanotechnology* (Ed.: C. M. Sotomayor Torres), Plenum, New York, **2004**.
[2] J. Turunen, F. Wyrovsky, *Diffractive Optics*, Akademie Verlag, Berlin, **1997**.
[3] M. Ibn-Elhaj, M. Schadt, *Nature* **2001**, *410*, 796.
[4] N. Stuzmann, T. A. Tervoort, K. Bastiaansen, P. Smith, *Nature* **2000**, *407*, 613.
[5] L. A. Liew, W. G. Zhang, L. N. An, S. Shah, R. L. Luo, Y. P. Liu, T. Cross, M. L. Dunn, V. Bright, J. W. Daily, R. Raj, K. Ansenth, *Am. Ceram. Soc. Bull.* **2001**, *80*, 25.
[6] R. Knitter, W. Bauer, D. Göhring, J. Hausselt, *Adv. Eng. Mater.* **2001**, *3*, 49.
[7] W. Bauer, R. Knitter, *J. Mater. Sci.* **2002**, *37*, 3127.
[8] T. V. Konomenko, V. V. Konomenko, V. I. Konov, S. M. Pimenov, S. V. Garnov, A. V. Tischenko, A. M. Prokhorov, A. V. Khomich, *Appl. Phys. A* **1999**, *68*, 99.
[9] Y. Fu, N. Kok, A. Brian, D. Xie, *Rev. Sci. Instrum.* **2003**, *74*, 3689.
[10] M. K. Kelly, O. Ambacher, B. Dahlheimer, G. Groos, R. Dimitrov, H. Angerer, M. Stutzmann, *Appl. Phys. Lett.* **1996**, *69*, 1749.
[11] T. Morita, K. Watanabe, R. Kometani, K. Kanda, Y. Haruyama, T. Taito, J.-i. Fujita, M. Ishida, Y. Ochiai, T. Tajima, S. Matsui, *Jpn. J. Appl. Phys.* **2003**, *42*, 3874.
[12] V. Oliveira, O. Conde, R. Vilar, *Adv. Eng. Mater.* **2001**, *3*, 75.
[13] Y. Hirayama, H. Yabe, M. Obara, *J. Appl. Phys.* **2001**, *89*, 2943.
[14] S. Y. Chou, P. R. Krauss, P. J. Renstrom, *Science* **1996**, *273*, 85.
[15] Y. Xia, G. M. Whitesides, *Angew. Chem.* **1998**, *110*, 568; *Angew. Chem. Int. Ed.* **1998**, *37*, 550.
[16] Y. Xia, J. A. Rogers, K. E. Paul, G. M. Whitesides, *Chem. Rev.* **1999**, *99*, 1823.
[17] B. Xu, F. Arias, G. M. Whitesides, *Adv. Mater.* **1999**, *11*, 492.
[18] M. Heule, S. Vuillemin, L. J. Gauckler, *Adv. Mater.* **2003**, *15*, 1237.
[19] H. Yang, P. Deschatelets, S. T. Brittain, G. M. Whitesides, *Adv. Mater.* **2001**, *13*, 54.
[20] W. S. Beh, Y. Xia, D. Qin, *J. Mater. Res.* **1999**, *14*, 3995.
[21] A. M. Xia, Y. Xia, J. J. McClelland, R. Gupta, D. Qin, X.-M. Zhao, L. L. Sohn, R. Celotta, G. M. Whitesides, *Adv. Mater.* **1997**, *9*, 147.
[22] R. Maboudian, W. R. Ashurst, C. Carraro, *Sens. Actuators A* **2000**, *82*, 219.
[23] F. Schreiber, *Prog. Surf. Sci.* **2000**, *65*, 151.
[24] O. Azzaroni, P. L. Schilardi, R. C. Salvarezza, *Nano Lett.* **2001**, *1*, 291.

[25] O. Azzaroni, P. L. Schilardi, R. C. Salvarezza, R. Gago, L. Vázquez, *Appl. Phys. Lett.* **2003**, *82*, 457.
[26] O. Azzaroni, M. H. Fonticelli, G. Benítez, P. L. Schilardi, R. Gago, I. Caretti, L. Vázquez, R. C. Salvarezza, *Adv. Mater.* **2004**, *16*, 405.
[27] S. P. Chenakin, *Vacuum* **2002**, *66*, 157, and references therein.
[28] Q. Zhao, M. Lukitsch, J. Xu, G. Auner, R. Niak, P.-K. Kuo, *MRS Internet J. Nitride Semicond. Res.* **2000**, *551*, W11.69.
[29] J. R. Mileham, S. J. Pearton, C. R. Abernathy, J. D. MacKenzie, R. J. Shul, S. P. Kilcoyne, *Appl. Phys. Lett.* **1995**, *67*, 1119.
[30] Y. Hirayama, H. Yabe, M. Obara, *J. Appl. Phys.* **2003**, *89*, 2943.
[31] O. Azzaroni, M. Cipollone, M. E. Vela, R. C. Salvarezza, *Langmuir* **2001**, *17*, 1483.
[32] M. A. Auger, R. Gago, M. Fernández, O. Sánchez, J. M. Albella, *Surf. Sci. Technol.* **2002**, *157*, 26.
[33] S. Seraji, Y. Wu, N. E. Jewel-Larson, M. J. Forbess, S. J. Limmer, T. P. Chou, G. Cao, *Adv. Mater.* **2000**, *12*, 1421.
[34] C. R. Martin, I. A. Aksay, *J. Phys. Chem. B* **2003**, *107*, 4261.
[35] Z. Zhang, F. F. Lange, *Adv. Eng. Mater.* **2002**, *4*, 294.
[36] Z. Yu, L. Chen, W. Wu, H. Ge, S.Y. Chou, *J. Vac. Sci. Technol. B* **2003**, *21*, 2089.
[37] U. P. Schönholzer, L. J. Gauckler, *Adv. Mater.* **1999**, *11*, 630.
[38] J. X. Gao, M. B. Chan-Park, D. Z. Xie, Y. H. Yan, W. X. Zhou, B. K. A. Ngoi, C. Y. Yue, *Chem. Mater.* **2004**, *16*, 956.
[39] M. A. Auger, O. Sánchez, C. Ballesteros, M. Jergel, M. Aguilar-Frutis, C. Falcony, *Thin Solid Films* **2003**, *433*, 211.
[40] M. Wittling, A. Benavid, P. J. Martin, M. V. Swain, *Thin Solid Films* **1995**, *270*, 283.
[41] T. G. Bifano, H. E. Fawcett, P. A. Bierden, *Precis. Eng.* **1997**, *20*, 53.
[42] J. M. Antunes, A. Cavaleiro, L. F. Menezes, M. I. Simoes, J. V. Fernández, *Surf. Coat. Technol.* **2002**, *149*, 27.
[43] J. Taniguchi, Y. Tokano, I. Miyamoto, M. Komuro, H. Hiroshima, *Nanotechnology* **2002**, *13*, 592.
[44] S. Y. Chou, C. Kelmel, J. Gu, *Nature* **2002**, *417*, 835.
[45] D. M. Dabbs, I. A. Aksay, *Annu. Rev. Phys. Chem.* **2000**, *51*, 601.
[46] M. Park, C. Harrison, P. M. Chaikin, R. A. Register, D. H. Adamson, *Science* **1997**, *276*, 1401.
[47] S. B. Clendenning, S. Aouba, M. S. Rayat, D. Grozea, J. B. Sorge, P. M. Brodersen, R. N. S. Sodhi, Z.-H. Lu, C. M. Yip, M. R. Freeman, H. E. Ruda, I. Manners, *Adv. Mater.* **2004**, *16*, 215.
[48] R. Gago, L. Vazquez, R. Cuerno, M. Varela, C. Ballesteros, J. M. Albella, *Appl. Phys. Lett.* **2001**, *78*, 3316.
[49] B. D. Gates, G. M. Whitesides, *J. Am. Chem. Soc.* **2003**, *125*, 14986.

Received: September 14, 2004

